Am J Transl Res 2025;17(7):5586-5601
www.ajtr.org /ISSN:1943-8141/AJTR0165261

Original Article

Development and validation of a gradient boosting machine-based model for predicting tumor-infiltrating lymphocyte proportions in breast cancer

Xiaobin Zhang, Shulin Xian, Daolai Huang, Naihan Cui, Jiehua Li

Department of Gastrointestinal Gland Surgery, The First Affiliated Hospital of Guangxi Medical University, Nanning 530021, Guangxi, China

Received April 11, 2025; Accepted July 15, 2025; Epub July 25, 2025; Published July 30, 2025

Abstract: Objective: To construct and validate a multidimensional model for evaluating tumor-infiltrating lymphocyte (TIL) levels in breast cancer (BC) patients. Methods: This retrospective study included 318 BC patients with 318 lesions confirmed by MRI and surgical pathology in the First Affiliated Hospital of Guangxi Medical University from January 2021 to December 2024. The patients were randomly split into a training set (n=228) and a validation (n=90) set, and further divided into low and high TIL groups based on immunophenotype assessment. Multivariate Logistic regression was used to identify independent predictors of TILs levels. A gradient boosting machine (GBM) model and a Logistic regression model were built. Model performance was assessed using receiver operating characteristic (ROC) curves, calibration curves, and decision curve analysis (DCA). An external validation cohort of 120 BC patients admitted between January 2025 and May 2025 was used to verify the predictive accuracy of the GBM model. Results Ki-67 level, internal enhancement pattern, multifocality, apparent diffusion coefficient (ADC) value, and neutrophil-to-lymphocyte ratio (NLR) were identified as independent predictors of high TIL levels. The GBM model demonstrated superior performance compared to the Logistic regression in the training set (AUC: 0.859 vs 0.724; P=0.014). Calibration curves indicated good agreement between predicted and observed probabilities in both models. DCA showed that the GBM model provided higher clinical utility. External validation yielded an AUC of 0.784 for the GBM model, with the calibration curve and DCA further confirming the model's good calibration and clinical applicability. Conclusion: The GBM-based multidimensional model reliably predicts TIL levels in BC patients, supporting prognosis evaluation and guiding personalized treatment strategies.

Keywords: Breast cancer, tumor infiltrating lymphocytes, multidimensional indicators, evaluation model

Introduction

Breast cancer (BC) is the most prevalent malignancy among women worldwide. According to the International Agency for Research on Cancer (IARC), 2.26 million new BC cases were reported in 2020, surpassing lung cancer as the most commonly diagnosed cancer [1, 2]. Its incidence continues to rise annually and exhibits a trend toward younger age groups, imposing a substantial burden on families and healthcare systems [3]. As understanding of BC pathophysiology deepens, tumor-infiltrating lymphocytes (TILs) - comprising T cells, B cells, and other immune subsets in the tumor microenvironment - have emerged as critical prognostic markers [4-6].

Studies have shown that high TIL levels correlate with improved disease-free survival (DFS) and overall survival (OS), particularly in triple-negative breast cancer (TNBC) and HER2-positive subtypes [7-9]. For example, TNBC patients with high TIL infiltration exhibit a 30% lower recurrence risk, as TILs directly mediate tumor cell cytotoxicity and inhibit metastasis [10, 11]. However, traditional pathological assessment of TIL via hematoxylin and eosin-stained sections is limited by inter-observer variability and subjective interpretation, resulting in inconsistent accuracy [12]. Recent advances in medical technology have enabled multi-dimensional solutions. Magnetic resonance imaging (MRI) provides quantitative parameters (e.g., apparent diffusion coefficient [ADC], vascular perme-

https://doi.org/10.62347/PDEW5000

ability) reflecting tumor microenvironment (TME) characteristics [13, 14]. In addition, systemic inflammatory markers from peripheral blood, such as neutrophil-lymphocyte ratio (NLR) and platelet-lymphocyte ratio (PLR), have been shown to correlate with immune status and tumor progression [15, 16].

Logistic regression is a widely used method due to its simplicity and interpretability, estimating the probability of binary outcomes based on linear combinations of variables [17]. However, it often underperforms in imbalanced datasets and lacks the flexibility to capture complex, non-linear relationships. In contrast, gradient boosting machines (GBM), an ensemble learning approach, build predictive models by iteratively fitting decision trees to the residuals of previous models, allowing accurate modeling of high-dimensional and non-linear data [18, 19].

Based on this, integrating multi-dimensional indicators to build an accurate model for predicting TIL levels holds significant clinical value. Such a model is expected to improve the accuracy and reliability of TIL assessment, reduce observer-related variability, and provide robust prognostic and therapeutic guidance. Furthermore, by exploring the intrinsic correlation between multi-dimensional indicators, it may enhance our understanding of TIL-related mechanisms in the TME and inform the development of novel immunotherapeutic strategies. The purpose of this study is to systematically integrate multi-dimensional parameters and construct a robust GBM-based model to predict TIL levels in BC patients.

Materials and methods

Research subjects

This retrospective study included 318 BC patients with 318 lesions who were treated at the First Affiliated Hospital of Guangxi Medical University between January 2021 and December 2024. In addition, another 120 BC patients admitted to our hospital between January 2024 and May 2025 were selected as the validation set to verify the predictive performance of the developed models.

Inclusion criteria: (1) Histopathologically confirmed invasive BC with complete pathological and immunohistochemical data; (2) Age >18 years; (3) Receipt of multiparametric MRI examination at the study center within two weeks prior to surgery; (4) Availability of histopathological assessment of TIL levels in surgical specimens. Exclusion criteria: (1) Receipt of preoperative neoadjuvant therapy; (2) Any breast-related treatment before MRI examination; (3) Poor MRI image quality precluding analysis; (4) Incomplete clinical or imaging data. This study was approved by the Ethics Committee of the First Affiliated Hospital of Guangxi Medical University.

Methods

Imaging protocol: Multi-parametric MRI was performed using a 1.5T MRI scanner (uMR 560, United Imaging) equipped with a dedicated 4-channel SENSE breast coil. Patients were positioned prone, with both breasts naturally suspended within the coil. Scanning sequences and parameters: T1WI (repetition time (TR)=4.8 ms, echo time (TE)=2.1 ms, matrix=320×320, slice thickness=3 mm), T2W1 (TR=3800 ms, TE=42.7 ms, matrix=328×350, slice thickness=4 mm), DWI (TR=3800 ms, TE=78.4 ms, matrix=350×200, slice thickness=4 mm, b=50 and 800 s/mm^2). Dynamic contrast-enhanced MRI (DCE-MRI): A high-resolution isotropic volume excitation (THRIVE) sequence was used with TR=5.1 ms, TE=2.1 ms, matrix=320×320, and slice thickness=2.4 mm. A pre-contrast mask image was acquired, followed by intravenous injection of gadopentetate dimeglumine at a dose of 0.2 ml/kg body weight using a power injector via the median cubital vein at a flow rate of 1.5 ml/s. This was immediately followed by a 20 ml normal saline flush at the same rate. Post-contrast images were obtained in six consecutive phases, each with a 60-second interval. ADC mapping was generated by single exponential fitting of DWI signals at b=50 and 800 s/mm^2, using the following formula: ADC=[lnS0-lnS (b)]/b, where S0 and S (b) represent the DWI signal intensity at b=50 and 800 s/mm^2, respectively.

MRI image analysis: According to the American College of Radiology Breast Imaging Reporting and Data System (ACR BI-RADS) standard [20], multi-parametric MRI images were evaluated. Two radiologists with 3 and 15 years of experience in breast MRI interpretation independent-

ly reviewed all images. Both were blinded to pathological outcomes. In cases of disagreement on qualitative assessments, consensus was reached through discussion. Quantitative measurements were analyzed to assess inter-observer consistency.

Lesions were categorized as either mass or non-mass enhancement (NME). When both types coexisted, the NME component was used to characterize the lesion. The MRI features evaluated included morphological features (lesion shape, margin, internal enhancement features), kinetic features (time-signal intensity curve (TIC) types), invasion of surrounding tissues (e.g., pectoralis muscle, skin, or nipple), axillary lymph nodes, multifocality/multicentricity, peritumoral edema, maximum lesion diameter, and ADC value.

TICs were classified into three types: persistent (type I), plateau (type II), and washout (type III). Surrounding tissue invasion was defined as clear imaging evidence of tumor extension into the pectoralis muscle, skin or nipple. Positive axillary lymph nodes were defined by one or more of the following: round or irregular shape, absent fatty hilum, cortical thickening, or short-axis diameter ≥10 mm. Multifocality was defined as multiple lesions within the same quadrant, while multicentricity referred to lesions located in different quadrants. Peritumoral edema was identified as a hyperintense signal on T2-weighted imaging surrounding or extending posterior to the tumor, consistent with fluid signal characteristics [21]. Measurement of maximum lesion diameter was performed on the image showing the most prominent enhancement. In cases of multiple lesions, the largest lesion was selected for analysis. ADC values were measured by placing a region of interest (ROI) (4-5 mm in diameter) within the area of lowest signal intensity on the ADC map (corresponding to the highest signal on DWI). ROI placement was guided by DCE-MRI and T2WI images to avoid necrotic zones, cystic components, or artifacts.

Clinical data collection and pathological data evaluation

Clinical and pathological data were collected for each patient, including age, menstrual status, lesion location, preoperative T stage, histopathological subtype, preoperative T stage, estrogen receptor (ER) status, progesterone receptor (PR) status, human epidermal growth factor receptor 2 (HER-2), and Ki-67 levels.

According to the 2010 American Society of Clinical Oncology/College of American pathologists (ASCO/CAP) guidelines [22], ER and PR positivity was defined as ≥1% of tumor nuclei exhibiting positive staining; <1% was defined as negative. HER-2 low expression was defined as HER-2 immunohistochemistry (IHC) score of 1 + or 2 + with negative fluorescence in situ hybridization (FISH); while high HER-2 expression was defined as HER-2 IHC score of 3 +, or 2 + with FISH positive results. Based on the 2013 St. Gallen International Expert Consensus [23], Ki-67<14% is defined as low expression, and Ki-67≥14% is defined as high expression.

Peripheral blood data were obtained from routine preoperative laboratory tests. Based on absolute neutrophil count, lymphocyte count, and platelet count, the following inflammatory indices were calculated: NLR, PLR, and systemic Immune-Inflammatory Index (SII).

Evaluation of TIL proportion

HE stained histological sections of surgical specimens were evaluated by designated pathologists according to the 2014 recommendations of the Breast Cancer International TILs Working Group [24]. The percentage of TILs was calculated under an optical microscope. The average value was defined as the percentage of stromal area within the tumor occupied by mononuclear immune cells, evaluated under a light microscope. The average value across fields was recorded as the TILs proportion for each sample. TILs <10% were defined as low TILs level, and the samples with TILs ≥10% were defined as high TILs level. In cases where the TIL proportion was uncertain, final classification was determined by consensus after consultation with senior pathologists.

Statistical methods

SPSS 29.0 was used for data analysis. Continuous variables with normal distribution were expressed as mean ± standard deviation (mean ± sd) and compared using the independent sample t-test. Non-normally distributed continuous variables were presented as median and interquartile range [M (P_{25}, P_{75})] and compared

using the Mann-Whitney U test. Categorical variables were presented in the form of percentage (%) and compared using the χ^2 test. Univariate and multivariate Logistic regression analysis was performed to identify factors associated with TILs levels in BC patients. Based on the selected variables, both a GBM model and a multivariate Logistic regression model were constructed. The relative importance of each clinical feature was obtained using GBM algorithm. The receiver operating characteristic (ROC) curve and calibration curve were used to evaluate the predictive efficacy of the models. Decision curve analysis (DCA) was used to evaluate the clinical applicability of both models. All tests were two-sided, with a significance level set at α=0.05.

Results

Comparison of multi-dimensional indicators between training set and validation set

A total of 318 BC patients were randomly divided into a training set (228 cases) and a validation set (90 cases) at a ratio of 7:3. No significant differences were observed between the two sets in terms of multidimensional indicators, including age, menstrual status, lesion location, preoperative T stage, histopathological subtype, ER status, PR status, HER-2 positivity, Ki-67 level, tumor shape and margin, internal enhancement pattern, TIC type, invasion of surrounding tissues, axillary lymph nodes, multifocality/multicentricity, peritumoral edema, ADC, molecular subtype, absolute neutrophil count, absolute lymphocyte count, PLT, NLR, PLR, SII (all P>0.05, **Table 1**).

General clinical data of the patients

Among the 318 BC patients included, the age range was 33-79 years. The low TIL group comprised 156 patients aged 33-78 years, with an average age of (53.01±9.65) years. The high TIL group included 162 patients aged 35-79 years, with an average of 54.09 (± 9.07) years. Significant differences were observed between the high and low TIL groups in terms of Ki-67 index, internal enhancement pattern, multifocality/multicentricity, ADC value, and NLR (all P<0.05, **Table 2**).

Univariate and multivariate Logistic regression analysis

Univariate Logistic regression analysis showed that Ki-67 index, internal enhancement patterns, multifocality/multicentricity, ADC value, NLR and SII were significantly associated with TIL levels in BC patients (P<0.05). According to the postoperative pathological results, TIL level was used as the dependent variable (0=low level, 1=high level), and variables with P<0.05 in univariate analysis were further included in a multivariate Logistic regression model. The results showed that Ki-67 index, internal enhancement patterns, multifocality/multicentricity, ADC value, and NLR were independently associated with high TIL levels in BC patients (P<0.05, **Table 3**).

Construction of a multivariate Logistic regression model for high TIL levels in BC patients based on multi-dimensional indicators

Based on the results of the multivariate Logistic regression analysis, a predictive model for high TIL levels in BC patients was constructed and visualized. The model incorporated Ki-67 index, internal enhancement characteristics, multifocality/multicentricity, ADC value, and NLR. The total score was mapped to a predicted probability of high TIL level in BC patients, as shown in **Figure 1**.

Validation of the Logistic regression model for predicting high TIL levels in BC patients

The performance of the Logistic regression model was evaluated using the ROC curve and calibration curve in both the training and validation sets. In the training set, the Logistic regression model achieved an AUC of 0.742 (95% CI: 0.678-0.805), with a sensitivity and specificity of 74.40% and 64.90%, respectively. In the validation set, the AUC was 0.674 (95% CI: 0.562-0.785), with a sensitivity and specificity of 51.10% and 82.20%, respectively (**Figure 2**). The calibration curves showed good agreement between the predicted probabilities and observed incidence of high TIL levels in both training and validation sets (**Figure 3**).

Construction of the GBM model for predicting high TIL levels in BC patients based on multi-dimensional indicators

Variables identified as significant in multivariate regression analysis were incorporated into the GBM model. The shrinkage rate was set to 0.005, and the initial number of boosting iterations (n. trees) was set to 5,000. A 10-fold cross-validation approach was used to determine the optimal number of trees. The mini-

Table 1. Comparison of multi-dimensional indicators between the training set and validation set

Index	Training set (n=228)	Verification set (n=90)	$t/\chi^2/Z$	P
Age (years)	53.62±9.44	53.40±9.20	0.191	0.849
Menstrual status [n (%)]			1.538	0.215
Premenopausal	99 (43.42)	46 (51.11)		
Postmenopausal	129 (56.58)	44 (48.89)		
Location of lesion [n (%)]			0.172	0.679
Left	97 (42.54)	36 (40.00)		
Right	131 (57.46)	54 (60.00)		
Histopathological subtype [n (%)]			1.898	0.168
Invasive carcinoma	190 (83.33)	69 (76.67)		
Other	38 (16.67)	21 (23.33)		
Preoperative T staging [n (%)]			2.184	0.535
T1	51 (22.37)	14 (15.56)		
T2	91 (39.91)	37 (41.11)		
T3	71 (31.14)	31 (34.44)		
T4	15 (6.58)	8 (8.89)		
ER [n (%)]			0.070	0.792
Negative	59 (25.88)	22 (24.44)		
Positive	169 (74.12)	68 (75.56)		
PR [n (%)]			0.589	0.443
Negative	66 (28.95)	30 (33.33)		
Positive	162 (71.05)	60 (66.67)		
HER2 [n (%)]			0.154	0.694
Negative	157 (68.86)	64 (71.11)		
Positive	71 (31.14)	26 (28.89)		
Ki-67 [n (%)]			0.106	0.744
<14%	31 (13.60)	11 (12.22)		
≥14%	197 (86.40)	79 (87.78)		
Tumor shape [n (%)]			0.081	0.776
Round/oval	67 (29.39)	25 (27.78)		
Irregular	161 (70.61)	65 (72.22)		
Tumor margin [n (%)]			0.757	0.384
Smooth	14 (6.14)	8 (8.89)		
Burr/Irregular	214 (93.86)	82 (91.11)		
Internal strengthening characteristics [n (%)]			0.762	0.683
Homogeneous strengthening	92 (40.35)	37 (41.11)		
Uneven strengthening	128 (56.14)	48 (53.33)		
Ring strengthening	8 (3.51)	5 (5.56)		
TIC curve [n (%)]			0.235	0.889
Type I	24 (10.53)	9 (1.00)		
Type II	178 (78.07)	69 (76.67)		
Type III	26 (11.40)	12 (13.33)		
Invasion of surrounding tissue [n (%)]			0.860	0.354
No	183 (80.26)	68 (75.56)		
Yes	45 (19.74)	22 (24.44)		
Axillary lymph nodes [n (%)]			0.029	0.865
Negative	104 (45.61)	42 (46.67)		
Positive	124 (54.39)	48 (53.33)		
Multifocal/multicenter [n (%)]			2.439	0.118
No	97 (42.54)	43 (47.78)		
Yes	131 (57.46)	47 (52.22)		

Peritumoral edema [n (%)]			0.367	0.544
No	113 (49.56)	48 (53.33)		
Yes	115 (50.44)	42 (46.67)		
ADC value	907.34±160.90	917.76±158.23	0.523	0.602
Molecular subtypes [n (%)]			0.053	0.817
Lumina type	140 (61.40)	54 (60.00)		
Non-Lumina type	88 (38.60)	36 (40.00)		
Neutrophil absolute value ($\times10^9$/L)	4.15±1.31	4.19±1.10	0.304	0.761
Lymphocyte absolute value ($\times10^9$/L)	1.20±0.37	1.23±0.41	0.638	0.524
Platelet count ($\times10^9$/L)	226.25±64.81	218.11±72.94	0.972	0.332
NLR	3.51 (2.45, 4.96)	3.57 (2.54, 3.99)	0.145	0.885
PLR	189.72 (141.20, 249.46)	182.01 (123.29, 250.59)	1.023	0.306
SII	743.02 (490.11, 1123.28)	727.31 (480.75, 1037.70)	0.621	0.534

Note: TILs, Tumor infiltrating lymphocytes; ER, Estrogen receptor; PR, progesterone receptor; HER-2, human epidermal growth factor receptor 2; TIC, Time-intensity curve; ADC, Apparent diffusion coefficient; NLR, Neutrophil-to-Lymphocyte Ratio; PLR, Platelet-to-Lymphocyte Ratio; SII, Systemic Immune-Inflammatory Index.

Table 2. Comparison of clinical data between the high and low TIL groups

Index	High TIL group (n=162)	Low TIL group (n=156)	$t/\chi^2/Z$	P
Age (years)	54.09±9.07	53.01±9.65	1.035	0.302
Menstrual status [n (%)]			0.001	0.976
Premenopausal	74 (45.68)	71 (45.51)		
Postmenopausal	88 (54.32)	85 (54.49)		
Location of lesion [n (%)]			0.261	0.610
Left	70 (43.21)	63 (40.38)		
Right	92 (56.79)	93 (59.62)		
Histopathological subtype [n (%)]			0.314	0.575
Invasive carcinoma	130 (70.25)	129 (82.69)		
Other	32 (19.75)	27 (17.31)		
Preoperative T staging [n (%)]			0.359	0.950
T1	35 (21.60)	30 (19.23)		
T2	64 (39.51)	64 (41.03)		
T3	52 (32.10)	50 (32.05)		
T4	116.79	12 (7.69)		
ER [n (%)]			0.340	0.560
Negative	39 (24.07)	42 (26.92)		
Positive	123 (75.93)	114 (73.07)		
PR [n (%)]				
Negative	51 (31.48)	45 (28.85)		
Positive	111 (68.52)	111 (71.15)		
HER2 [n (%)]			1.157	0.282
Negative	117 (72.22)	104 (66.67)		
Positive	45 (27.78)	52 (33.33)		
Ki-67 [n (%)]			9.691	0.002
<14%	12 (7.41)	30 (19.23)		
≥14%	150 (92.59)	126 (80.77)		
Tumor shape [n (%)]			0.001	0.974
Round/oval	47 (29.01)	45 (28.85)		
Irregular	115 (70.98)	111 (71.15)		
Tumor margin [n (%)]			0.285	0.593
Smooth	10 (6.17)	12 (7.69)		
Burr/Irregular	152 (93.83)	144 (92.31)		

Internal strengthening characteristics [n (%)]			7.840	0.021
Homogeneous strengthening	102 (62.96)	75 (48.08)		
Uneven strengthening	54 (33.33)	74 (47.44)		
Ring strengthening	6 (3.70)	7 (4.49)		
TIC curve [n (%)]			3.015	0.221
Type I	15 (9.26)	18 (11.54)		
Type II	132 (81.48)	115 (73.72)		
Type III	15 (9.26)	23 (14.74)		
Invasion of surrounding tissue [n (%)]			0.344	0.558
No	130 (80.25)	121 (77.56)		
Yes	32 (19.75)	35 (22.44)		
Axillary lymph nodes [n (%)]			1.465	0.26
Negative	69 (42.59)	77 (47.53)		
Positive	93 (57.40)	79 (48.77)		
Multifocal/multicenter [n (%)]			6.883	0.009
No	77 (47.53)	97 (62.18)		
Yes	85 (52.47)	59 (37.82)		
Peritumoral edema [n (%)]			0.052	0.819
No	81 (50.00)	80 (51.28)		
Yes	81 (50.00)	76 (47.72)		
ADC value	949.95±162.73	869.11±146.55	4.649	<0.001
Molecular subtypes [n (%)]			1.234	0.267
Lumina type	94 (58.02)	100 (64.10)		
Non-Lumina type	68 (41.98)	56 (35.90)		
Neutrophil absolute value ($\times 10^9$/L)	4.27±1.47	4.04±9.66	1.644	0.101
Lymphocyte absolute value ($\times 10^9$/L)	1.18±0.37	1.25±0.39	1.650	0.100
Platelet count ($\times 10^9$/L)	222.31±63.54	225.63±70.96	0.440	0.660
NLR	1.18±0.37	1.25±0.39	4.075	<0.001
PLR	192.33 (141.85, 267.69)	177.12 (137.18, 237.00)	-1.251	0.224
SII	741.18 (465.26, 1332.49)	735.74 (522.33, 950.61)	-1.000	0.317

Note: TILs, Tumor infiltrating lymphocytes; ER, Estrogen receptor; PR, progesterone receptor; HER-2, human epidermal growth factor receptor 2; TIC, Time-intensity curve; ADC, Apparent diffusion coefficient; NLR, Neutrophil-to-Lymphocyte Ratio; PLR, Platelet-to-Lymphocyte Ratio; SII, Systemic Immune-Inflammatory Index.

mum generalization error was achieved when n.trees =1035 (**Figure 4A**). L2 regularization was added by default, implemented by adding the squared sum of model parameters to the loss function to prevent overfitting. The relative importance of each clinical feature obtained by GBM was NLR, ADC, Ki-67 index, multifocality/multicentricity, and internal reinforcement pattern, in descending order (**Figure 4B**).

Validation of the GBM model for predicting high TIL levels in BC patients based on multi-dimensional indicators

The ROC curve and calibration curve were generated to assess the performance of the GBM model in both the training and the validation sets. In the training set, the GBM model achieved an ACU of 0.859 (95% CI: 0.810-0.908), with sensitivity and specificity of 74.40% and 85.60%, respectively. In the validation set, the AUC was 0.683 (95% CI: 0.573-0.794), and the sensitivity and specificity were 48.90% and 80.00%, respectively (**Figure 5**). The calibration curves showed that the predicted probabilities of the GBM model closely matched the actual incidence of high TIL levels in both datasets, indicating good calibration and predictive consistency of the GBM model (**Figure 6**).

Comparison of prediction efficiency between the GBM model and Logistic regression model

Delong test results showed that the ACU of GBM model in the training set was significantly higher than that of the Logistic regression model (Z=-2.456, P=0.014). In the validation

Table 3. Univariate and multivariate Logistic regression analysis for high TIL levels

Variable	Single factor analysis		multiple-factor analysis	
	OR (95% CI)	*P*	OR (95% CI)	*P*
Age	1.031 (0.989-1.037)	0.301	-	-
Menstrual status	0.993 (0.639-1.545)	0.976	-	-
Location of lesion	0.890 (0.570-1.391)	0.610	-	-
Histopathological subtype	0.575 (0.482-1.499)	0.850	-	-
Preoperative T staging	0.946 (0.733-1.221)	0.670	-	-
ER status	1.162 (0.701-1.925)	0.560	-	-
PR status	0.882 (0.546-1.425)	0.609	-	-
HER2 status	0.769 (0.477-1.241)	0.283	-	-
Ki-67 index	2.976 (1.463-6.054)	0.003	3.127 (1.446-6.761)	0.004
Mass shape	0.992 (0.611-1.611)	0.974	-	-
Mass edge	1.267 (0.531-3.022)	0.594	-	-
Internal strengthening characteristics	1.569 (1.052-2.340)	0.027	1.651 (1.069-2.550)	0.024
TIC curve	0.866 (0.543-1.381)	0.546	-	-
Invasion of surrounding tissue	0.851 (0.496-1.460)	0.558	-	-
Axillary lymph nodes	1.314 (0.844-2.044)	0.226	-	-
Multifocal/multicenter	1.815 (1.161-2.838)	0.009	1.836 (1.122-3.004)	0.016
Peritumoral edema	1.053 (0.678-1.634)	0.819	-	-
Tumor length	0.924 (0.798-1.071)	0.296	-	-
ADC value	1.003 (1.002-1.005)	<0.001	1.003 (1.001-1.005)	<0.001
Molecular subtypes	0.774 (0.493-1.217)	0.267	-	-
Neutrophils	1.160 (0.971-1.385)	0.102	-	-
Lymphocytes	0.614 (0.343-1.099)	0.101	-	-
PLT	0.999 (0.996-1.003)	0.659	-	-
NLR	1.252 (1.117-1.404)	<0.001	1.329 (1.098-1.610)	0.004
PLR	1.001 (0.999-1.003)	0.448	-	-
SII	1.000 (1.000-1.001)	0.020	1.000 (0.999-1.000)	0.429

Note: TILs, Tumor infiltrating lymphocytes; ER, Estrogen receptor; PR, progesterone receptor; HER-2, human epidermal growth factor receptor 2; TIC, Time-intensity curve; ADC, Apparent diffusion coefficient; NLR, Neutrophil-to-Lymphocyte Ratio; PLR, Platelet-to-Lymphocyte Ratio; SII, Systemic Immune-Inflammatory Index.

set, however, there was no significant difference in ACU between the two models (Z=-0.061, P=0.951) (**Table 4**).

Clinical applicability of the GBM model for predicting high TIL levels in BC

DCA analyses of the GBM model and multivariate Logistic regression model are shown in **Figures 7**, **8**. In the training set, the GBM model demonstrated a higher net benefit than the Logistic regression model across most threshold probabilities, indicating superior clinical utility. Although both models showed reduced net benefit at high-risk thresholds, the GBM model exhibited a slower decline in net benefit, suggesting greater stability when stricter risk classification is required. Moreover, the training and validation set curves of the GBM model were more closely aligned, indicating better generalization capability and more consistent performance on new data. These findings suggest that the GBM model is more suitable for clinical application and offers broader practical utility than the Logistic regression model.

External validation and clinical implementation of the GBM model

Among the 120 patients in the external validation set, there were 58 patients with low TIL levels and 62 with high TIL levels. The GBM model was applied using the five previously identified predictors: Ki-67 index, internal enhancement pattern, multifocality/multicentricity, ADC value, and NLR. The ROC curve yielded an AUC of 0.784 (95% CI: 0.703-0.865), indicating strong discriminatory power of the

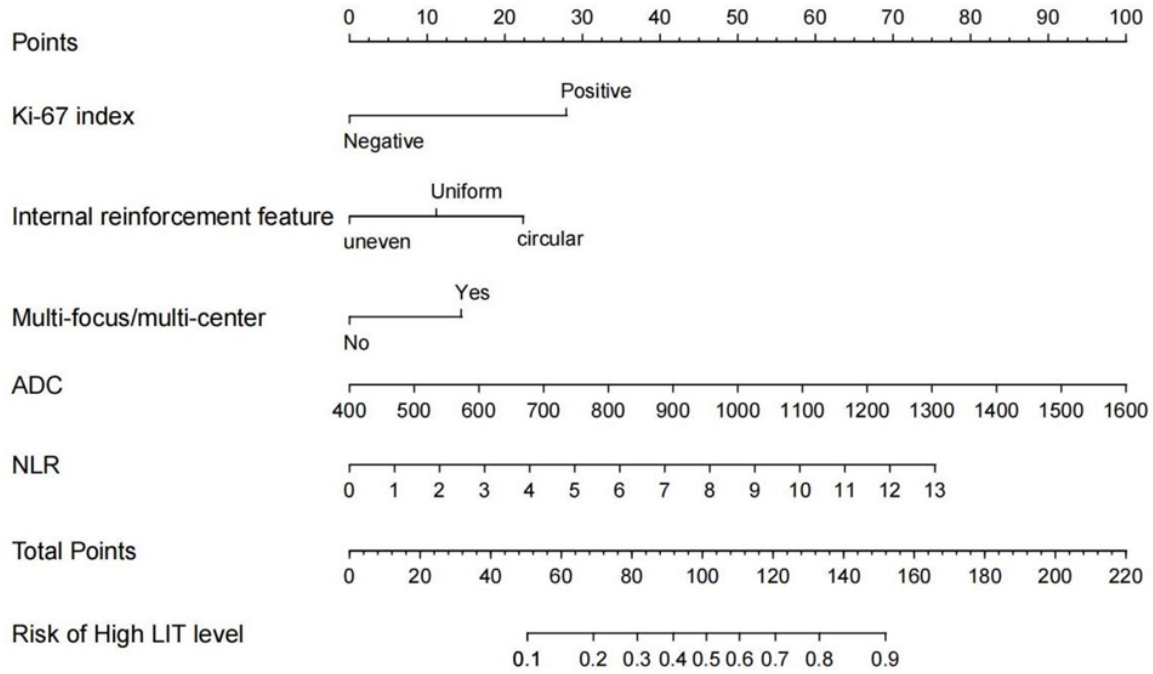

Figure 1. Construction of a multivariate Logistic regression model for predicting high TIL levels in breast cancer patients. ADC, Apparent diffusion coefficient; NLR, Neutrophil-to-Lymphocyte ratio.

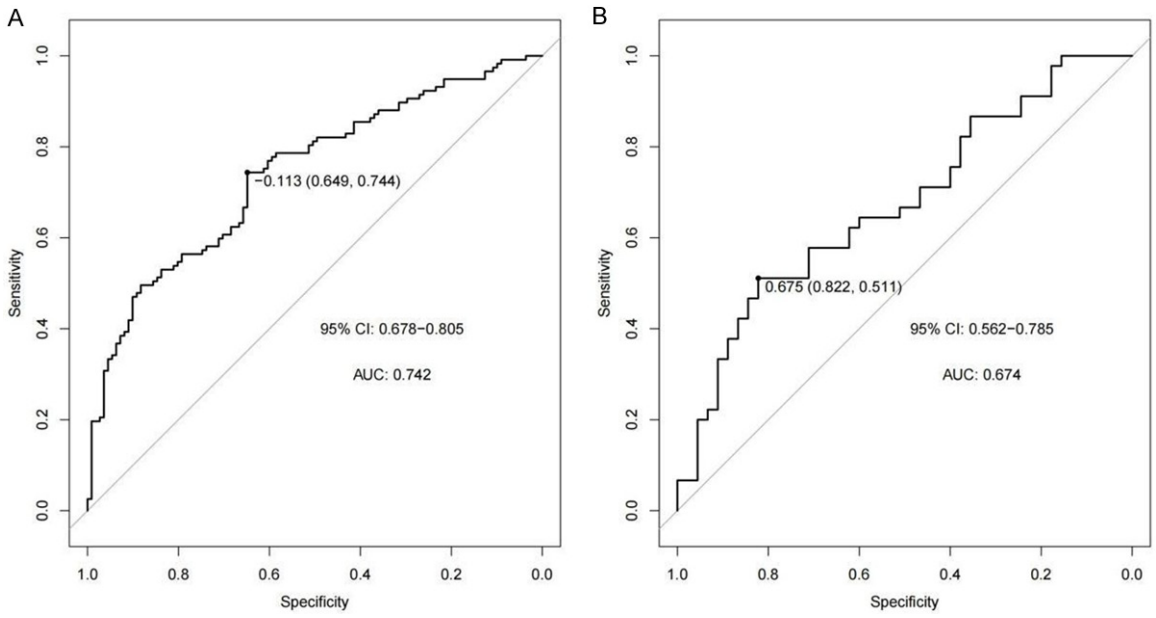

Figure 2. ROC curves for Logistic regression model in predicting high TIL levels in BC patients. A. Training set; B. Validation set; ROC, Receiver operating characteristic; TILs, Tumor-infiltrating lymphocytes; BC, Breast cancer.

GBM model (**Figure 9A**). The calibration curve demonstrated good agreement between predicted and observed probabilities (**Figure 9B**). The decision curve showed that the model provided consistent net clinical benefit (**Figure 9C**).

Discussion

Tumor-infiltrating lymphocytes (TILs) are a subset of lymphocytes predominantly composed of T cells, including CD4 + T lymphocytes, CD8 + T

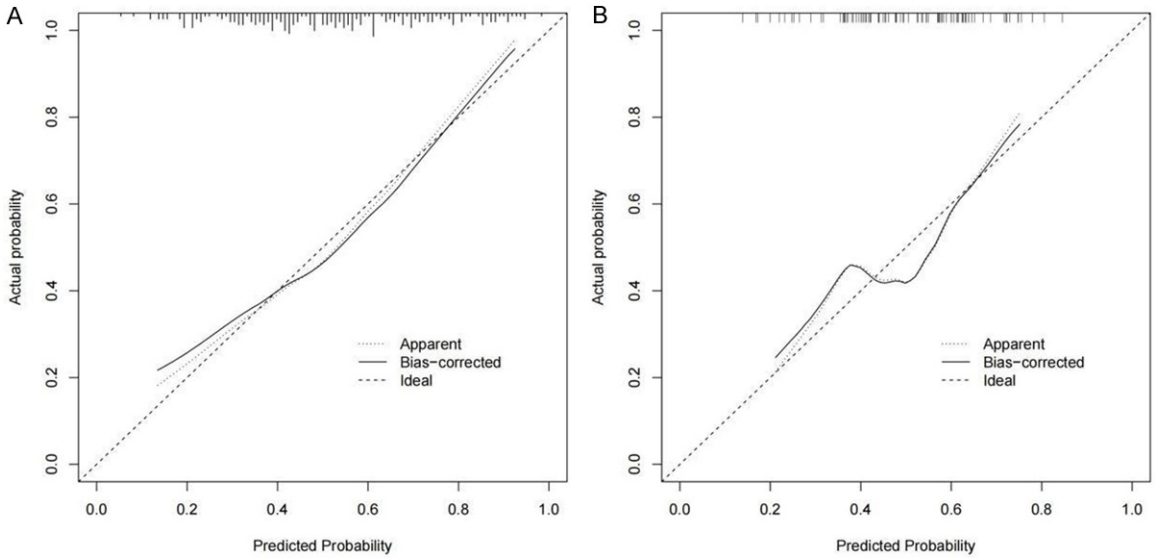

Figure 3. Calibration curves for Logistic regression model in predicting high TIL levels in BC patients. A. Training set; B. Validation set; TILs, Tumor-infiltrating lymphocytes; BC, Breast cancer.

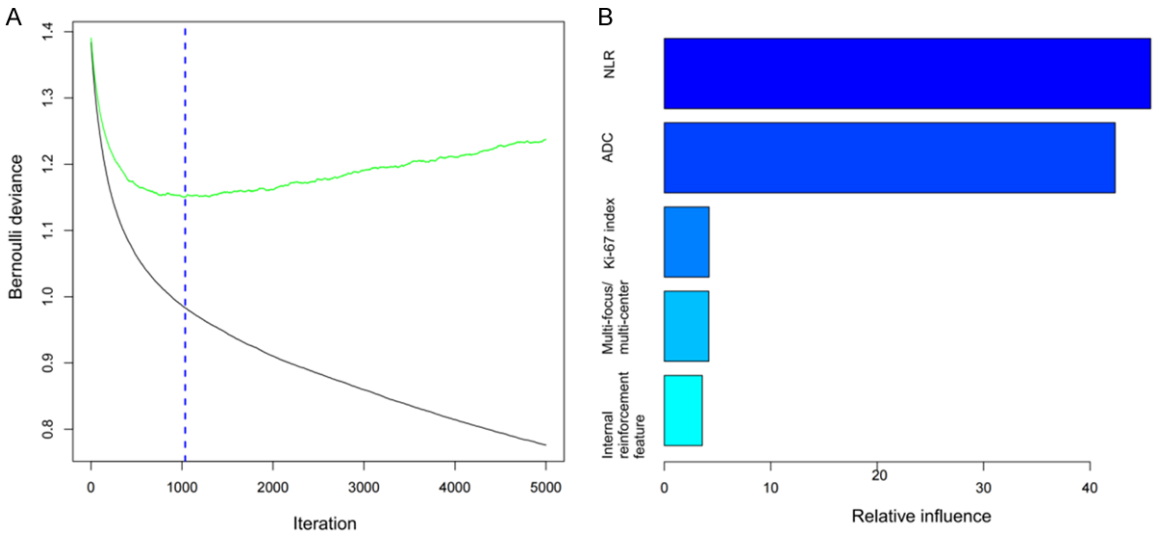

Figure 4. GBM model optimization and variable contribution analysis in predicting TIL levels. A. The graph of iteration times and error rate; B. The relative importance of ranking of variables in the GBM model; ADC, Apparent diffusion coefficient; NLR, Neutrophil-to-Lymphocyte ratio; GBM, Gradient Boosting machine.

lymphocytes, and regulatory T lymphocytes. These immune cells are particularly abundant in TNBC and HER-2 positive BCs. TILs have been recognized as independent prognostic biomarkers associated with favorable prognosis and are increasingly being integrated into diagnostic practice [25]. TILs reflect the immune landscape of the TME and play a key role in modulating anti-tumor immunity. They have shown utility in guiding personalized immunotherapy, monitoring therapeutic responses, and predicting clinical prognosis. Previous studies indicate that evaluating TIL levels helps identify BC patients who may be more responsive to immune modulation and neoadjuvant chemotherapy, enabling timely adjustments to treatment strategies and promoting individualized therapy [13, 26-28].

This study found statistically significant differences in the Ki-67 index, internal enhancement characteristics, multifocality/multicen-

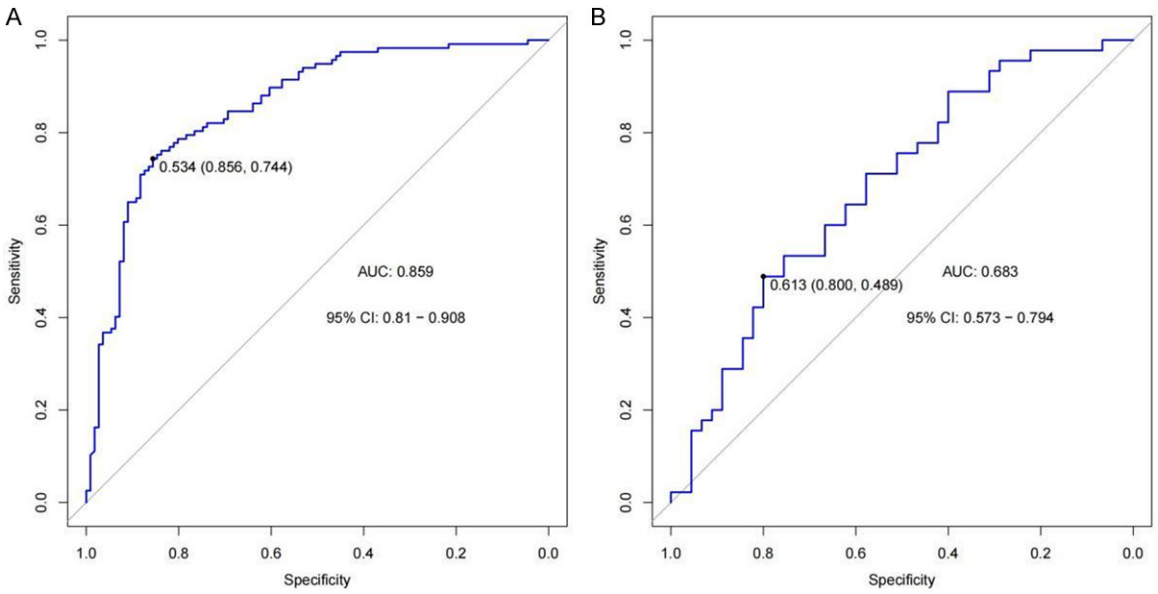

Figure 5. ROC curves for GBM model in predicting high TIL levels in BC patients. A. training set; B. Validation set; ROC, Receiver operating characteristic; TILs, Tumor-infiltrating lymphocytes; BC, Breast cancer; GBM, Gradient Boosting machine.

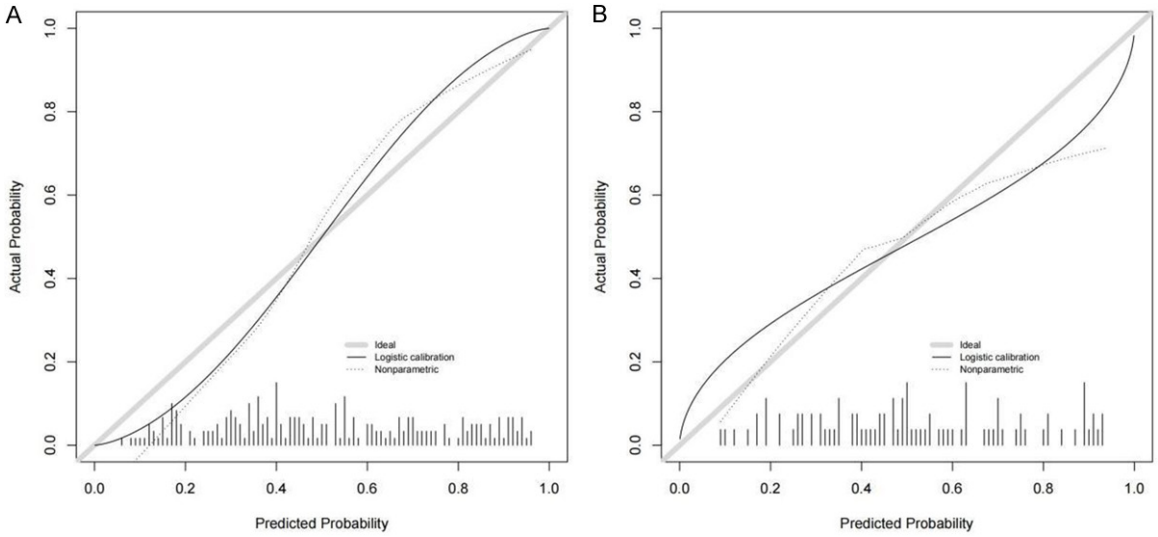

Figure 6. Calibration curves for the GBM model in predicting high TIL levels in BC patients. A. Training set; B. Validation set; TILs, Tumor-infiltrating lymphocytes; BC, Breast cancer; GBM, Gradient Boosting machine.

Table 4. Comparison of predictive efficiency between the GBM model and Logistic regression model

Indicators	GBM model		Logistic regression model	
	Training set	Validation set	Training set	Validation set
AUC	0.859	0.683	0.724	0.674
Specificity	0.856	0.800	0.649	0.822
Sensitivity	0.744	0.489	0.774	0.511
Accuracy	0.767	0.589	0.658	0.578

Note: AUC, Area under the curve; GBM, Gradient Boosting machine.

tricity, ADC value, and NLR between the high and low TIL groups. The observed positive correlation between high Ki-67 expression and TIL level is consistent with its role in tumor cell proliferation. Elevated Ki-67 may enhance tumor antigen presentation, activate immune responses, and promote T cell infiltration. This

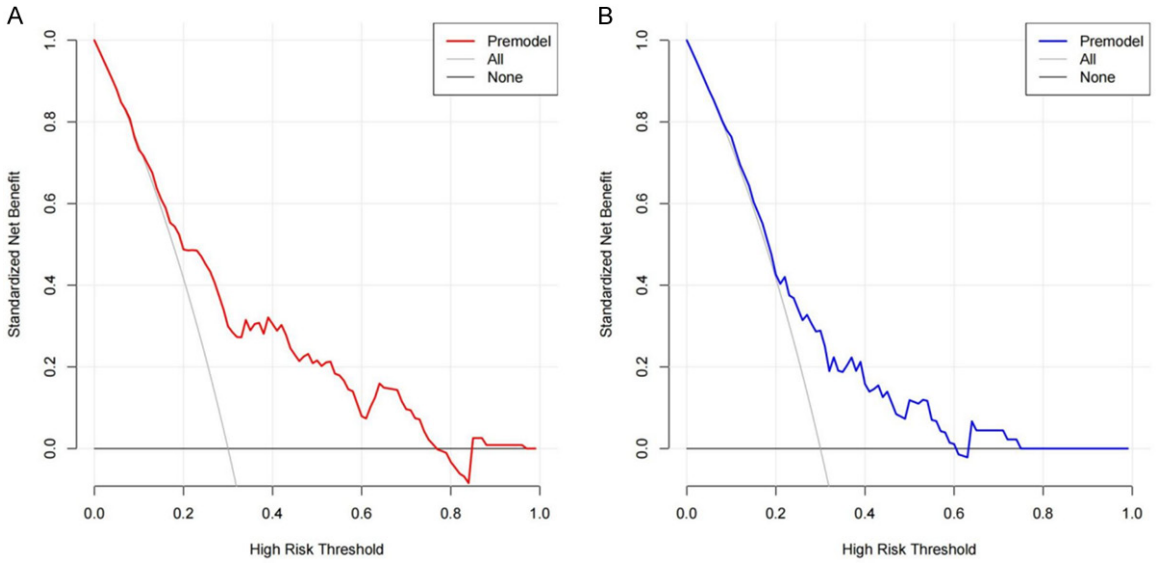

Figure 7. Decision curve analysis for the Logistic regression model in predicting high TIL levels in BC patients. A. Training set; B. Validation set; TILs, Tumor-infiltrating lymphocytes; BC, Breast cancer.

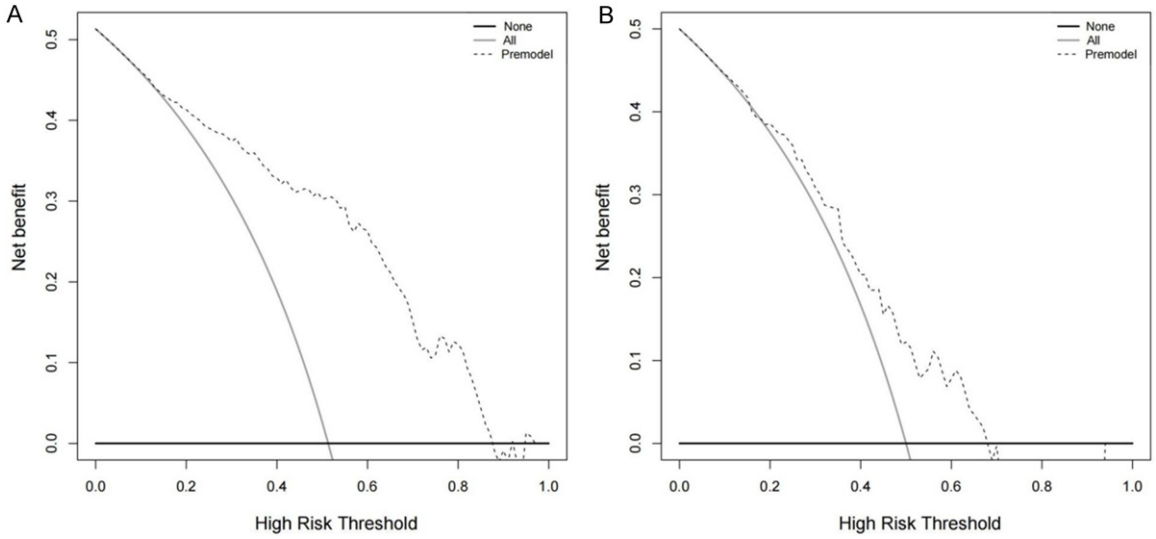

Figure 8. Decision curve analysis for the GBM model in predicting high TIL levels in BC patients. A. Training set; B. Validation set; TILs, Tumor-infiltrating lymphocytes; BC, Breast cancer; GBM, Gradient Boosting machine.

indicates that highly proliferative tumors can trigger stronger immune surveillance, thereby facilitating TIL aggregation. Celebi et al. [29] and Ku et al. [30] reported that lesions with high TIL levels often exhibited more homogeneous internal enhancement patterns, which is consistent with our findings. Biologically, this may relate to the reduced collagen fibers content in TIL-rich tumors, which permits more uniform contrast agent distribution. Collagen fibers can hinder the migration of immune cells, and their density is negatively correlated with TILs infiltration, thereby linking imaging features to tumor immunophenotype [31, 32]. Contrary to a previous report linking solitary lesions to high TILs in TNBC [30], our study revealed that multifocal/multicentric tumors were more frequently associated with elevated TILs. This discrepancy may stem from differences in molecular subtypes across cohorts. Multifocal lesions may exhibit increased immunogenic heterogeneity, potentially stimulating

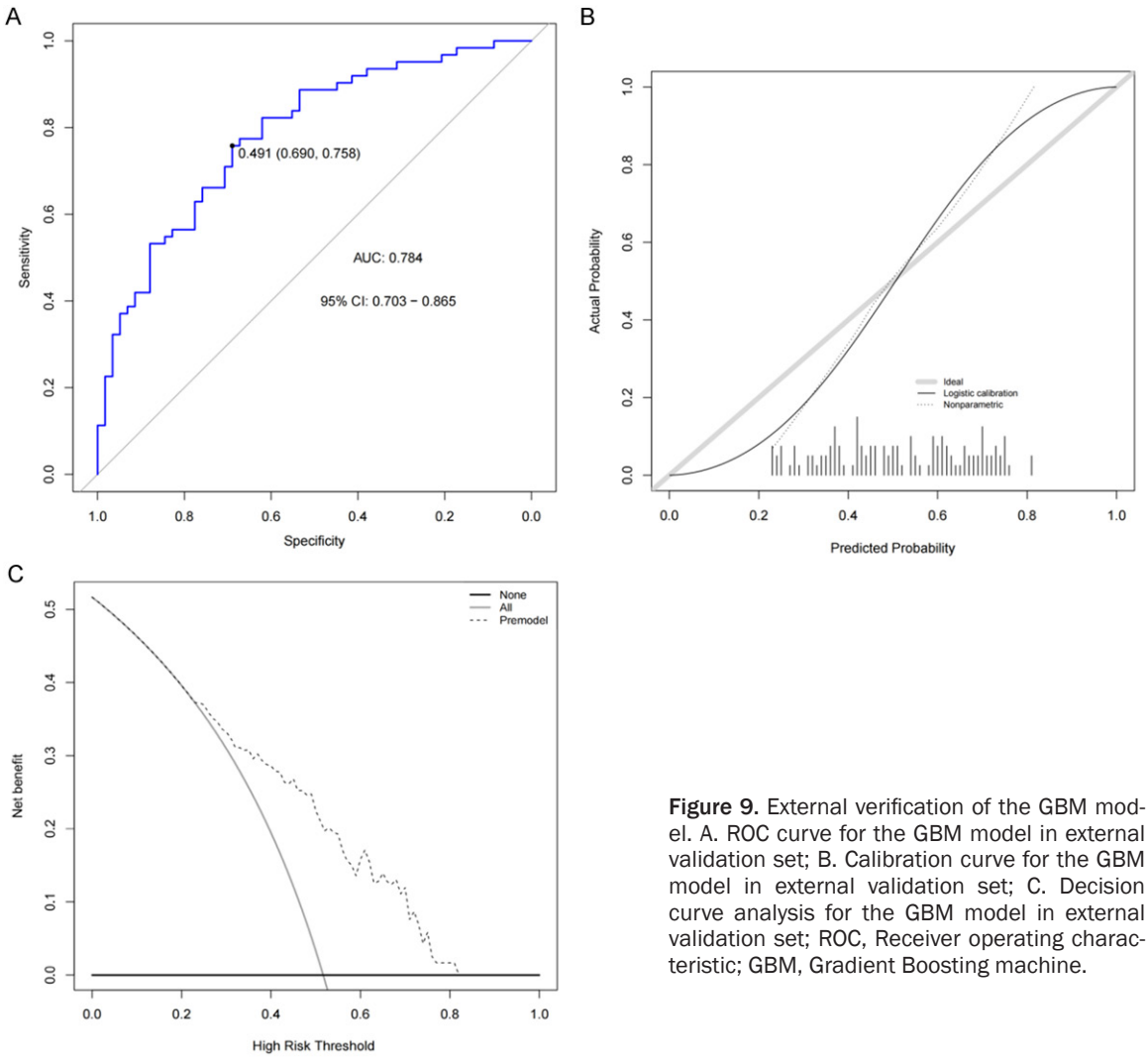

Figure 9. External verification of the GBM model. A. ROC curve for the GBM model in external validation set; B. Calibration curve for the GBM model in external validation set; C. Decision curve analysis for the GBM model in external validation set; ROC, Receiver operating characteristic; GBM, Gradient Boosting machine.

systemic immune activation and promoting widespread TIL recruitment.

High TILs levels were also associated with increased ADC values, which reflect water molecule diffusion within the TME. Compared with tumor cells, TILs possess higher cytoplasmic fluidity and stronger water molecule diffusion ability, contributing to elevated ADC measurements. Variability in mean ADC values in the literature [29, 33] may result from differences in ROI location, scanning parameters, and tumor cell density. The negative correlation between NLR and TIL levels underscores the effect of systemic inflammation on local antitumor immunity. Neutrophils inhibit TIL infiltration by promoting the Treg cell differentiation and inducing CD8 + T cell apoptosis [34-36]. As an easy-to-obtain biomarker, NLR serves as a bridge between systemic inflammation and tumor immune status, providing clinical value in predicting immune-related outcomes.

In this study, Ki-67 index, internal enhancement features, multifocality/multicentricity, ADC value, and NLR were included as predictors in both the GBM and Logistic regression models. However, the models differ markedly in feature utilization. The GBM sorts the predictors by importance based on iterative residual learning, capturing nonlinear interactions (NLR > ADC > Ki-67 > multifocality > internal enhancement features) [37]; however, Logistic regression relies on a linear hypothesis, providing interpretable odds ratios, but potentially underestimating the complex relationship, which explains its relatively low predictive performance [38].

This study demonstrated that the GBM model outperformed the Logistic regression model in the training set (AUC: 0.859 vs. 0.724), showing stronger multidimensional data analysis capabilities. In the validation set, the two models showed comparable performance (AUC: 0.683 vs 0.674). Decision curve analysis showed that the GBM model provided a higher net benefit across most threshold probabilities, especially in the training set, and it is more stable in the validation set, suggesting that it has higher clinical utility across a variety of clinical scenarios. In addition, the application of the GBM model to an external validation cohort demonstrated an accuracy of 83.33% in identifying patients with high TIL levels, indicating strong predictive performance and potential for clinical application.

This study's retrospective design and single-center data introduces selection bias and restricts generalizability. Additionally, the relatively small sample size may compromise statistical power. Future research should prioritize multicenter, prospective studies with larger, diverse cohorts. Incorporating emerging biomarkers (e.g., immune checkpoint molecules) and multi-omics data may further optimize predictive accuracy and enhance the clinical applicability of TIL-based prognostic models in breast cancer.

Conclusion

In summary, Ki-67 index, internal enhancement characteristics, multifocality/multicentricity, ADC value, and NLR are significantly associated with high TIL levels in breast cancer. Based on these multi-dimensional indicators, the GBM model demonstrate good predictive efficacy and clinical practicability, offering a valuable tool for prognosis evaluation and facilitating individualized treatment of BC patients.

Disclosure of conflict of interest

None.

Address correspondence to: Jiehua Li, Department of Gastrointestinal Gland Surgery, The First Affiliated Hospital of Guangxi Medical University, Nanning 530021, Guangxi, China. Tel: +86-0771-5350100; E-mail: drlijiehua1978@163.com

References

[1] Sung H, Ferlay J, Siegel RL, Laversanne M, Soerjomataram I, Jemal A and Bray F. Global cancer statistics 2020: GLOBOCAN estimates of incidence and mortality worldwide for 36 cancers in 185 countries. CA Cancer J Clin 2021; 71: 209-249.

[2] Giaquinto AN, Sung H, Miller KD, Kramer JL, Newman LA, Minihan A, Jemal A and Siegel RL. Breast cancer statistics, 2022. CA Cancer J Clin 2022; 72: 524-541.

[3] Kashyap D, Pal D, Sharma R, Garg VK, Goel N, Koundal D, Zaguia A, Koundal S and Belay A. Global increase in breast cancer incidence: risk factors and preventive measures. Biomed Res Int 2022; 2022: 9605439.

[4] Leon-Ferre RA, Jonas SF, Salgado R, Loi S, de Jong V, Carter JM, Nielsen TO, Leung S, Riaz N, Chia S, Jules-Clement G, Curigliano G, Criscitiello C, Cockenpot V, Lambertini M, Suman VJ, Linderholm B, Martens JWM, van Deurzen CHM, Timmermans AM, Shimoi T, Yazaki S, Yoshida M, Kim SB, Lee HJ, Dieci MV, Bataillon G, Vincent-Salomon A, Andre F, Kok M, Linn SC, Goetz MP, Michiels S; International Immuno-Oncology Biomarker Working Group. Tumor-infiltrating lymphocytes in triple-negative breast cancer. JAMA 2024; 331: 1135-1144.

[5] Ciarka A, Piatek M, Peksa R, Kunc M and Senkus E. Tumor-Infiltrating Lymphocytes (TILs) in breast cancer: prognostic and predictive significance across molecular subtypes. Biomedicines 2024; 12: 763.

[6] Wu R, Oshi M, Asaoka M, Yan L, Benesch MGK, Khoury T, Nagahashi M, Miyoshi Y, Endo I, Ishikawa T and Takabe K. Intratumoral Tumor Infiltrating Lymphocytes (TILs) are associated with cell proliferation and better survival but not always with chemotherapy response in breast cancer. Ann Surg 2023; 278: 587-597.

[7] Angelico G, Broggi G, Tinnirello G, Puzzo L, Vecchio GM, Salvatorelli L, Memeo L, Santoro A, Farina J, Mule A, Magro G and Caltabiano R. Tumor Infiltrating Lymphocytes (TILS) and PD-L1 expression in breast cancer: a review of current evidence and prognostic implications from pathologist's perspective. Cancers (Basel) 2023; 15: 4479.

[8] Huertas-Caro CA, Ramirez MA, Rey-Vargas L, Bejarano-Rivera LM, Ballen DF, Nunez M, Mejia JC, Sua-Villegas LF, Cock-Rada A, Zabaleta J, Fejerman L, Sanabria-Salas MC and Serrano-Gomez SJ. Tumor infiltrating lymphocytes (TILs) are a prognosis biomarker in Colombian patients with triple negative breast cancer. Sci Rep 2023; 13: 21324.

[9] Su GH, Xiao Y, Jiang L, Zheng RC, Wang H, Chen Y, Gu YJ, You C and Shao ZM. Radiomics features for assessing tumor-infiltrating lymphocytes correlate with molecular traits of triple-negative breast cancer. J Transl Med 2022; 20: 471.
[10] Schlam I, Loi S, Salgado R and Swain SM. Tumor-infiltrating lymphocytes in HER2-positive breast cancer: potential impact and challenges. ESMO Open 2025; 10: 104120.
[11] Michaels E, Chen N and Nanda R. The role of immunotherapy in Triple-Negative Breast Cancer (TNBC). Clin Breast Cancer 2024; 24: 263-270.
[12] Rizzo A and Ricci AD. Biomarkers for breast cancer immunotherapy: PD-L1, TILs, and beyond. Expert Opin Investig Drugs 2022; 31: 549-555.
[13] Bian T, Wu Z, Lin Q, Mao Y, Wang H, Chen J, Chen Q, Fu G, Cui C and Su X. Evaluating tumor-infiltrating lymphocytes in breast cancer using preoperative MRI-based radiomics. J Magn Reson Imaging 2022; 55: 772-784.
[14] Haodong G, Jianguo Z, Pylypenko D, Weiqiang D, Sheng S, Jie X and Haige L. Ultrafast dynamic contrast-enhanced breast MRI with quantitative perfusion parameters in differentiating breast cancer: a study focusing on triple-negative and HER2 positive breast cancer. Front Oncol 2025; 14: 1457918.
[15] Kumarasamy C, Tiwary V, Sunil K, Suresh D, Shetty S, Muthukaliannan GK, Baxi S and Jayaraj R. Prognostic utility of platelet-lymphocyte ratio, neutrophil-lymphocyte ratio and monocyte-lymphocyte ratio in head and neck cancers: a detailed PRISMA compliant systematic review and meta-analysis. Cancers (Basel) 2021; 13: 4166.
[16] Eastern Rectal Cancer Response Collaborative, Ireland. A multicentre cohort study assessing the utility of routine blood tests as adjuncts to identify complete responders in rectal cancer following neoadjuvant chemoradiotherapy. Int J Colorectal Dis 2022; 37: 957-965.
[17] Chhatwal J, Alagoz O, Lindstrom MJ, Kahn CE Jr, Shaffer KA and Burnside ES. A Logistic regression model based on the national mammography database format to aid breast cancer diagnosis. AJR Am J Roentgenol 2009; 192: 1117-1127.
[18] Rodriguez-Tomas E, Arenas M, Baiges-Gaya G, Acosta J, Araguas P, Malave B, Castane H, Jimenez-Franco A, Benavides-Villarreal R, Sabater S, Sola-Alberich R, Camps J and Joven J. Gradient boosting machine identified predictive variables for breast cancer patients pre- and post-radiotherapy: preliminary results of an 8-year follow-up study. Antioxidants (Basel) 2022; 11: 2394.
[19] Wang H, Zhang C, Li Q, Tian T, Huang R, Qiu J and Tian R. Development and validation of prediction models for papillary thyroid cancer structural recurrence using machine learning approaches. BMC Cancer 2024; 24: 427.
[20] Lee KA. Breast imaging reporting and data system category 3 for magnetic resonance imaging. Top Magn Reson Imaging 2014; 23: 337-344.
[21] Lee HJ, Lee JE, Jeong WG, Ki SY, Park MH, Lee JS, Nah YK and Lim HS. HER2-positive breast cancer: association of MRI and clinicopathologic features with tumor-infiltrating lymphocytes. AJR Am J Roentgenol 2022; 218: 258-269.
[22] Hammond ME, Hayes DF, Dowsett M, Allred DC, Hagerty KL, Badve S, Fitzgibbons PL, Francis G, Goldstein NS, Hayes M, Hicks DG, Lester S, Love R, Mangu PB, McShane L, Miller K, Osborne CK, Paik S, Perlmutter J, Rhodes A, Sasano H, Schwartz JN, Sweep FC, Taube S, Torlakovic EE, Valenstein P, Viale G, Visscher D, Wheeler T, Williams RB, Wittliff JL and Wolff AC. American Society of Clinical Oncology/College Of American Pathologists guideline recommendations for immunohistochemical testing of estrogen and progesterone receptors in breast cancer. J Clin Oncol 2010; 28: 2784-2795.
[23] Goldhirsch A, Winer EP, Coates AS, Gelber RD, Piccart-Gebhart M, Thurlimann B, Senn HJ; Panel members. Personalizing the treatment of women with early breast cancer: highlights of the St Gallen international expert consensus on the primary therapy of early breast cancer 2013. Ann Oncol 2013; 24: 2206-2223.
[24] Salgado R, Denkert C, Demaria S, Sirtaine N, Klauschen F, Pruneri G, Wienert S, Van den Eynden G, Baehner FL, Penault-Llorca F, Perez EA, Thompson EA, Symmans WF, Richardson AL, Brock J, Criscitiello C, Bailey H, Ignatiadis M, Floris G, Sparano J, Kos Z, Nielsen T, Rimm DL, Allison KH, Reis-Filho JS, Loibl S, Sotiriou C, Viale G, Badve S, Adams S, Willard-Gallo K and Loi S; International TWG 2014. The evaluation of tumor-infiltrating lymphocytes (TILs) in breast cancer: recommendations by an International TILs Working Group 2014. Ann Oncol 2015; 26: 259-271.
[25] Denkert C, von Minckwitz G, Darb-Esfahani S, Lederer B, Heppner BI, Weber KE, Budczies J, Huober J, Klauschen F, Furlanetto J, Schmitt WD, Blohmer JU, Karn T, Pfitzner BM, Kummel S, Engels K, Schneeweiss A, Hartmann A, Noske A, Fasching PA, Jackisch C, van Mackelenbergh M, Sinn P, Schem C, Hanusch C, Untch M and Loibl S. Tumour-infiltrating lymphocytes and prognosis in different subtypes of breast cancer: a pooled analysis of 3771 patients

treated with neoadjuvant therapy. Lancet Oncol 2018; 19: 40-50.
[26] Qian XL, Xia XQ, Li YQ, Jia YM, Sun YY, Song YM, Xue HQ, Hao YF, Wang J, Wang XZ, Liu CY, Zhang XM, Zhang LN and Guo XJ. Effects of tumor-infiltrating lymphocytes on nonresponse rate of neoadjuvant chemotherapy in patients with invasive breast cancer. Sci Rep 2023; 13: 9256.
[27] Zhang B, Wang X and Cheng C. The ratio of intratumour to stromal infiltrating lymphocytes better predicts prognosis in breast cancer. Clin Transl Med 2023; 13: e1265.
[28] Agarwal G, Vishvak Chanthar KMM, Katiyar S, Kumari N, Krishnani N, Sabaretnam M, Chand G, Mishra A and Lal P. Predictive and prognostic role of tumor-infiltrating lymphocytes in patients with advanced breast cancer treated with primary systemic therapy. World J Surg 2023; 47: 1238-1246.
[29] Celebi F, Agacayak F, Ozturk A, Ilgun S, Ucuncu M, Iyigun ZE, Ordu C, Pilanci KN, Alco G, Gultekin S, Cindil E, Soybir G, Aktepe F and Ozmen V. Usefulness of imaging findings in predicting tumor-infiltrating lymphocytes in patients with breast cancer. Eur Radiol 2020; 30: 2049-2057.
[30] Ku YJ, Kim HH, Cha JH, Shin HJ, Baek SH, Lee HJ and Gong G. Correlation between MRI and the level of tumor-infiltrating lymphocytes in patients with triple-negative breast cancer. AJR Am J Roentgenol 2016; 207: 1146-1151.
[31] Candelaria RP, Spak DA, Rauch GM, Huo L, Bassett RL, Santiago L, Scoggins ME, Guirguis MS, Patel MM, Whitman GJ, Moulder SL, Thompson AM, Ravenberg EE, White JB, Abuhadra NK, Valero V, Litton J, Adrada BE and Yang WT. BI-RADS ultrasound lexicon descriptors and stromal tumor-infiltrating lymphocytes in triple-negative breast cancer. Acad Radiol 2022; 29 Suppl 1: S35-S41.
[32] Fukui K, Masumoto N, Shiroma N, Kanou A, Sasada S, Emi A, Kadoya T, Yokozaki M, Arihiro K and Okada M. Novel tumor-infiltrating lymphocytes ultrasonography score based on ultrasonic tissue findings predicts tumor-infiltrating lymphocytes in breast cancer. Breast Cancer 2019; 26: 573-580.
[33] Fogante M, Tagliati C, De Lisa M, Berardi R, Giuseppetti GM and Giovagnoni A. Correlation between apparent diffusion coefficient of magnetic resonance imaging and tumor-infiltrating lymphocytes in breast cancer. Radiol Med 2019; 124: 581-587.
[34] Wang H, Zhang H, Wang Y, Brown ZJ, Xia Y, Huang Z, Shen C, Hu Z, Beane J, Ansa-Addo EA, Huang H, Tian D and Tsung A. Regulatory T-cell and neutrophil extracellular trap interaction contributes to carcinogenesis in non-alcoholic steatohepatitis. J Hepatol 2021; 75: 1271-1283.
[35] Sadeghalvad M, Mohammadi-Motlagh HR and Rezaei N. Immune microenvironment in different molecular subtypes of ductal breast carcinoma. Breast Cancer Res Treat 2021; 185: 261-279.
[36] Song M, Zhang C, Cheng S, Ouyang D, Ping Y, Yang J, Zhang Y, Tang Y, Chen H, Wang QJ, Li YQ, He J, Xiang T, Zhang Y and Xia JC. DNA of neutrophil extracellular traps binds TMC06 to Impair CD8+ T-cell immunity in hepatocellular carcinoma. Cancer Res 2024; 84: 1613-1629.
[37] Holm CE, Grazal CF, Raedkjaer M, Baad-Hansen T, Nandra R, Grimer R, Forsberg JA, Petersen MM and Skovlund Soerensen M. Development and comparison of 1-year survival models in patients with primary bone sarcomas: external validation of a Bayesian belief network model and creation and external validation of a new gradient boosting machine model. SAGE Open Med 2022; 10: 20503121221076387.
[38] Guan C, Ma F, Chang S and Zhang J. Interpretable machine learning models for predicting venous thromboembolism in the intensive care unit: an analysis based on data from 207 centers. Crit Care 2023; 27: 406.